THE JOURNAL OF BIOLOGICAL CHEMISTRY VOL. 289, NO. 26, pp. 18033–18044, June 27, 2014

Repression of *Cyclin D1* Expression Is Necessary for the Maintenance of Cell Cycle Exit in Adult Mammalian Cardiomyocytes*

Received for publication, December 11, 2013, and in revised form, May 2, 2014 Published, JBC Papers in Press, May 12, 2014, DOI 10.1074/jbc.M113.541953

Shoji Tane[‡], Misae Kubota[§], Hitomi Okayama[‡], Aiko Ikenishi[‡], Satoshi Yoshitome[‡1], Noriko Iwamoto[‡2], Yukio Satoh[‡], Aoi Kusakabe[§], Satoko Ogawa[§], Ayumi Kanai[‡], Jeffery D. Molkentin[¶], Kazuomi Nakamura[‖], Tetsuya Ohbayashi[‖], and Takashi Takeuchi[‡§3]

From the [‡]School of Life Sciences, Faculty of Medicine, [‖]Division of Laboratory Animal Science, Research Center for Bioscience and Technology, Tottori University, Yonago 683-8503, Japan, [§]Mitsubishi Kagaku Institute of Life Sciences, Machida 194-8511, Japan, and [¶]Cincinnati Children's Hospital Medical Center, University of Cincinnati, Howard Hughes Medical Institute, Cincinnati, Ohio 45229

Background: How cell cycle exit is maintained in adult mammalian cardiomyocytes is largely unknown.
Results: Cyclin D1 expression causes cell cycle reentry in >40% of adult mouse cardiomyocytes.
Conclusion: Silencing the cyclin D1 expression is necessary for the maintenance of the cell cycle exit.
Significance: One of the mechanisms regulating cell cycle exit in mammalian cardiomyocytes has been uncovered.

The hearts of neonatal mice and adult zebrafish can regenerate after injury through proliferation of preexisting cardiomyocytes. However, adult mammals are not capable of cardiac regeneration because almost all cardiomyocytes exit their cell cycle. Exactly how the cell cycle exit is maintained and how many adult cardiomyocytes have the potential to reenter the cell cycle are unknown. The expression and activation levels of main cyclin-cyclin-dependent kinase (CDK) complexes are extremely low or undetectable at adult stages. The nuclear DNA content of almost all cardiomyocytes is 2C, indicating the cell cycle exit from G_1-phase. Here, we induced expression of cyclin D1, which regulates the progression of G1-phase, only in differentiated cardiomyocytes of adult mice. In these cardiomyocytes, S-phase marker-positive cardiomyocytes and the expression of main cyclins and CDKs increased remarkably, although cyclin B1-CDK1 activation was inhibited in an ATM/ATR-independent manner. The phosphorylation pattern of CDK1 and expression pattern of *Cdc25* subtypes suggested that a deficiency in the increase in *Cdc25* (*a* and *-b*), which is required for M-phase entry, inhibited the cyclin B1-CDK1 activation. Finally, analysis of cell cycle distribution patterns showed that >40% of adult mouse cardiomyocytes reentered the cell cycle by the induction of cyclin D1. The cell cycle of these binucleated cardiomyocytes was arrested before M-phase, and many mononucleated cardiomyocytes entered endoreplication. These data indicate that silencing the cyclin D1 expression is necessary for the maintenance of the cell cycle exit and suggest a mechanism that involves inhibition of M-phase entry.

Cardiomyocytes (CMs)[4] are essential for cardiac functions. If many CMs are lost and the loss is not recovered, heart failure or lethality occurs. The neonatal mouse and adult zebrafish are able to recover the loss of CMs after injury through proliferation of preexisting CM and thus regenerate their hearts (1–3). In contrast, adult mammals are not capable of substantial cardiac regeneration.

Recent studies have shown that postnatal CMs proliferate in normal mammals (4, 5). However, the percentages are very limited and insufficient to restore cardiac function after injury (at most, 0.06% per day in injured mice) (5).

These facts indicate that the cell cycle exit is strictly maintained in the majority of adult CMs. This raises two questions. How is the cell cycle exit maintained? How many adult CMs have the potential to reenter the cell cycle? Answers to these questions will contribute to regenerative medicine in the heart because reproliferation of many CMs enables substantial cardiac regeneration.

To address these questions, we have focused on cell cycle regulation in the mouse heart. The mitotic indices in CMs, and the expression and activation levels of main cyclin-CDK complexes (cyclin D-CDK4/6, cyclin E-CDK2, cyclin A-CDK1/2, and cyclin B-CDK1) in the hearts are high during early embryonic stages. These levels decrease from midgestation to birth and then show one wave in which the peak is around postnatal day 5 (P5) (6–9). The wave mainly produces binucleated cells from mononucleated cells. Eighty to ninety percent of CMs become binucleated cells (7, 9). Then all expression and activation levels of main cyclin-CDK complexes become extremely

* This work was supported in part by a research grant from the Ministry of Education, Culture, Sports, Science, and Technology of Japan (KAKEN Grants 19057011 and 25113520).
[1] Present address: Faculty of Pharmacy, Iwaki Meisei University, Iwaki 970-8511, Japan.
[2] Present address: Kinutani Women's Clinic, Hiroshima 730-0035, Japan.
[3] To whom correspondence should be addressed: School of Life Sciences, Faculty of Medicine, Tottori University, Yonago 683-8503, Japan. Tel.: 81-859-38-6231; Fax: 81-859-38-6233; E-mail: takeuchi@med.tottori-u.ac.jp.

[4] The abbreviations used are: CM, cardiomyocyte; CDK, cyclin-dependent kinase; ATM, ataxia telangiectasia mutated; ATR, AT- and RAD3-related; P, postnatal day; NLS, nuclear localizing signal; *CCD*, *CAG:loxP-CAT-polyA-loxP-NLS-cyclinD1-IRES-EGFP*; *MER*, *Myh6:MERCreMER*; *Myh6*, myosin heavy chain 6 gene; Tam, tamoxifen; PCNA, proliferating cell nuclear antigen; pH3-S10, phospho-histone H3-Ser-10; EdU, 5-ethynyl-2′-deoxyuridine; d.p.i., days post-injection; Rb, retinoblastoma protein; H2AX, histone H2A variant X; EGFP, enhanced GFP.

low or undetectable after P14, and the levels are maintained for life. Simultaneously, almost all CMs exit the cell cycle, and the state is strictly maintained. The nuclear DNA content of almost all CMs is 2C (6, 9), showing the cell cycle exit from G_1-phase.

Generally, the G_1 cell cycle progression is regulated by D-type cyclins-CDK4/6 complexes (10). D-type cyclins are regarded as sensors of the extracellular environment that link the mitogenic pathways to the core cell cycle machinery (11). One of these cyclin, cyclin D1, is required for repression of CM proliferation at mid-gestation (8). Expression of D-type cyclins as well as other main cyclins in the mouse hearts is very low after P14 (7–9).

In the present study we induced expression of cyclin D1 only in differentiated CMs of adult mice to reactivate the cyclin D-CDK4/6 complex and examined the effects on cell cycle progression. We found that >40% of adult CMs reentered the cell cycle due to the induction, indicating that silencing the cyclin D1 expression is necessary for the maintenance of the cell cycle exit.

EXPERIMENTAL PROCEDURES

Vector Construction—The CCD vector was produced by insertion of the nucleotide sequence for HA tag and nuclear localizing signal (NLS)-cyclin D1-internal ribosome entry site (IRES)-EGFP into the cloning site of a plasmid containing CAG promoter-loxP-*CAT*-loxP-cloning site-poly(A) (pBSKISecI CAG-CAT-Poly(A), a kind gift from Dr. Saga, National Institute of Genetics, Japan). The nucleotide sequence for NLS was tagged to the cyclin D1 transgene, because nuclear import of cyclin D1 is inhibited in rat neonatal and most likely adult CMs (12). That of HA was also tagged to the cyclin D1 transgene.

Mice—Mice with C3H/HeJ Jcl genetic backgrounds were used in all experiments other than experiments using $p21^{Cip1}$ KO mice. Original *MER* (*Myh6: MERCreMER*) (13) mice were backcrossed with C3H/HeJ mice. *MER* mice have been frequently used in CM-specific gene expression or knock-out studies and also in labeling differentiated CMs (14). The *CCD* transgenic mouse lines (*CAG:loxP-CAT-poly(A)-loxP-NLS-cyclinD1-IRES-EGFP*) were produced using the CCD vector, as described previously (15). The *CCD* (+)/*MER* (+) double-hemizygote mice were generated by intercrossing between *CCD* (+) and *MER* (+) mice. *CCD* (+)/*MER* (+); $p21^{Cip1-/-}$ mice were obtained by multiple crossing of *CCD* (+), *MER* (+), and $p21^{Cip1+/-}$ (a kind gift from Dr. Leder, Harvard University; C57BL/6 J) mice. Adult mice >6 weeks old were used in this study. For CM-specific induction of *NLS-cyclin D1* and *EGFP*, tamoxifen (Tam, Sigma) was dissolved at 10 mg/ml in corn oil (Sigma), and adult *CCD* (+)/*MER* (+) mice were administered 0.1 ml of dissolved Tam into the peritoneal cavity. The expression of transgenes by Cre recombination was confirmed by EGFP expression. The presence of a vaginal plug was regarded as E0.5. All mice were genotyped by PCR. All animals were handled and maintained in accordance with institutional guidelines (Animal Care and Use Committee, Tottori University) and the Guidelines for Proper Conduct of Animal Experiments (Science Council of Japan).

Histology and Immunostaining—The immunostaining was performed as described in previous reports (16–18). Frozen sections were used with the antibodies shown in Table 1. EGFP fluorescence was not detected in sections derived from *CCD* (+)/*MER* (+) mice with administration of Tam, most likely because of the fixation procedure. For analyses of cyclin D1-, BrdU-, Ki67-, and PCNA-positive CMs, frozen sections of the hearts were stained with each antibody (Table 1) using an immunofluorescence method. After these images were photographed, the same sections were stained with an antibody to Nkx2.5 (nuclear marker of CM; Table 1) using a peroxidase-labeled antibody method, because signals for Nkx2.5 are very weak at adult stages. The photographed images were merged, and positive CM (%) was determined from the number of double-positive cells/number of Nkx2.5 positive cells × 100. >1000 Nkx2.5 positive cells per mouse were counted. CMs were also identified by staining with an antibody to sarcomeric actin (Table 1). BrdU was injected 24 h before sampling. For analyses of phosphohistone H3-Ser-10 (pH3-S10), cardiac sections were coimmunostained with antibodies against cyclin D1 and pH3-S10. Because signals for Nkx2.5 in pH3-S10 positive nuclei are very weak, cyclin D1 was used as a marker for cardiomyocytes. Images were acquired with microscopes (AxioImager M1, Carl Zeiss) equipped with imaging software (AxioVision 4.8, Carl Zeiss) at room temperature. A microscopy camera (AxioCam MRc5, Carl Zeiss) was used for immunofluorescence staining and immunohistochemistry.

TABLE 1
Antibodies used in this study
WB, Western blotting; IP; immunoprecipitation; IF, Immunofluorescence; IHC, Immunohistochemistry.

Antigens	Antibodies	Assays
α-Sarcomeric actin	5C5; Sigma	IF
BrdU	ab6326; Abcam	IF
Cdc25a	sc7389; Santa Cruz Biotechnology	WB
Cdc25b	sc327; Santa Cruz Biotechnology	WB
CDK1	sc-54; Santa Cruz Biotechnology	WB
CDK2	sc-163; Santa Cruz Biotechnology	WB, IP
CDK4	sc-260; Santa Cruz Biotechnology	WB, IP
Cdt1	A gift from Dr. Hideo Nishitanai (Univ. Hyogo)	WB
Chk1	sc-8408; Santa Cruz Biotechnology	WB
Cyclin A	sc-751; Santa Cruz Biotechnology	IP
Cyclin A	CY-A1; Sigma	WB
Cyclin B1	GNS1; Thermo	IP
Cyclin B1	V152; Cell Signaling Technology	WB
Cyclin D1	SP4; Lab Vision	WB, IF
Cyclin E	07–683; Millipore	WB, IP
γ-H2AX	2577; Cell Signaling Technology	WB
GAPDH	sc-32233; Santa Cruz Biotechnology	WB
Geminin	A gift from Dr. Keiko Nakayama (Tohoku Univ.)	WB
H2AX	07–627; Millipore	WB
Ki-67	ab15580; Abcam	IF
Mcm3	ab4460; Abcam	WB
Mcm4	A gift from Dr. Hideo Nishitanai (Univ. Hyogo)	WB
Nkx2.5	sc-8657; Santa Cruz Biotechnology	IHC
$p21^{Cip1}$	SX118; BD Pharmingen	WB
$p27^{Kip1}$	G173–524; BD Pharmingen	WB
$p57^{Kip2}$	P0357; Sigma	WB
p53	sc-6243; Santa Cruz Biotechnology	WB
pCDK1-Y15	9111; Cell Signaling Technology	WB
pCDK2-T160	2561; Cell Signaling Technology	WB
pChk1-S345	2341; Cell Signaling Technology	WB
PCNA	sc-56; Santa Cruz Biotechnology	IF
pH3-S10	06–570; Millipore	IF

Enzymatic Dissociation of CMs into Single Cells and Measurement of DNA Content on Slide Glasses—Enzymatic dissociation of CMs of the cardiac ventricles into single cells was performed as described previously (9, 19). 1 mg/20 g body

TABLE 2
Primers for real-time RT-PCR

Gene	Forward primer	Reverse primer
Cdc25a	AAGAACCCTATTGTGCCTACTG	CATACAGCTCAGGGTAGTGG
Cdc25b	TCCACTGTGAATTCTCGTCTG	ATGCTGTGGGAAGAACTCC
Cdc25c	AGTCAGAAGGAACTGCATGAG	CAGAGAACGGCACATTCGAG
CDK1	CAGAGATTGACCAGCTCTT	GAAAGGTGTTCTTGTAGTCC
CDK2	CCAGGAGTTACTTCTATGCC	ATAGTGCAGCATTTGCGA
cyclin A2	CCTGCCTTCACTCATTGCTG	GTGGCGCTTTGAGGTAGGT
cyclin B1	CTATCCTACAGTGAAGACTC	TGCTTAGATGCTGCATAC
cyclin B2	GAGAGTGAAGTCCTGGAA	GTGCTGATCTTCAGGAGT
cyclin E1	GTGTCAAATGGATGGTTC	GGAGAAATCCTATTCTGTTC
cyclin E2	TGCATTCTAGCCATCGAC	GCACCATCCAGTCTACAC
GAPDH	GGGTGGAGCCAAAAGGGTCATC	GCCAGTGAGCTTCCCGTTCAGC

weight of EdU was injected into Tam-treated *CCD* (+)/*MER* (+) mice at 5 days post-injection (d.p.i.) for analysis at 7 d.p.i. or at both 5 and 7 d.p.i. for analysis at 14, 28, or 91 d.p.i. Dissociated CMs were fixed with 4% paraformaldehyde at 4 °C for 24 h. The CMs were washed once with distilled water and then smeared on slide glasses. EdU incorporation was detected as described previously (20). CMs were identified by staining with an antibody to sarcomeric actin (Table 1), as described in the histological methods (18). DNA was stained with 1 μg/ml DAPI for 30 min. After staining, fluorescence images were acquired with microscopes (BZ-9000, Keyence) equipped with imaging software (Viewer BZ-II, Keyence) at room temperature. A microscopy camera in BZ-9000 was used. Then DNA content per nucleus of CMs was measured with a Cell Cycle Application Module of MetaMorph software (Molecular Devices). The cell cycle distribution patterns of mono- and binucleated CMs was analyzed independently. We analyzed 1500–2000 nuclei of total and binucleated CMs and 100–200 nuclei of mononucleated CMs.

Western Blot Analysis, Immunoprecipitation, and in Vitro Kinase Assay for CDKs—The cardiac ventricles were lysed, and then immunoprecipitation, Western blot analysis, and *in vitro* kinase assays for CDKs were performed as described previously (9, 18, 21, 22). Antibodies used for immunoprecipitation and Western blot analysis are shown in Table 1. The intensity of the bands in Western blot analysis or *in vitro* kinase assay was quantified using Image J.

Real Time PCR—Real-time RT-PCR was performed as described previously (8). Primers are shown in Table 2. To standardize the amount of sample cDNA, *GAPDH* was used as an endogenous control.

Statistical Analysis—The experimental data were analyzed using Student's *t* test. Tukey's multiple comparison test was used after obtaining a significant difference with one-way analysis of variance for multiple comparison tests.

RESULTS

Induction of Cyclin D1 Only in Adult CMs—To investigate whether the reactivation of the cyclin D-CDK4/6 complex promoted the cell cycle reentry of adult mouse CMs *in vivo*, we induced expression of cyclin D1 only in differentiated adult CMs using an inducible Cre-loxP system (Fig. 1*A*). Expression of cyclin D1 and EGFP was induced in the hearts of double transgenic mice (*CCD* (+)/*MER* (+)) by a single administration of Tam (Fig. 1, *B–E*). Induction of cyclin D1 was observed in almost all *CCD* (+)/*MER* (+) CMs, as >95% of the CM marker, Nkx2.5-positive nuclei, were also positive for exogenous cyclin D1 at 7 d.p.i. (Fig. 1*C*). These cells were also positive for sarcomeric actin (data not shown). Conversely, all exogenous cyclin D1-positive cells were also positive for Nkx2.5 and sarcomeric actin. These data indicated that cyclin D1 induction was limited to CMs. In addition, the cyclin D-CDK4 activity increased in the hearts of *CCD* (+)/*MER* (+) mice after administration of Tam and was maintained constantly from at least 5 d.p.i. (Fig. 1*F*).

Increase in Proliferation Marker-positive CMs by Cyclin D1 Induction—We examined the effects of cyclin D1 induction on the cell cycle progression in adult CMs with immunostaining using antibodies against three cell proliferation markers (BrdU, Ki-67, and PCNA) in sections of hearts. The percentages of positive CMs with these markers increased significantly at 7 d.p.i. in *CCD* (+)/*MER* (+) mice when compared with control mice (Fig. 2*A*). Especially, >40% of CMs were positive with PCNA (Fig. 2, *A* and *B*). These proliferation marker-positive CMs were uniformly distributed in whole ventricles.

We next examined CMs in M-phase. An extremely low number of CMs (4–8 nuclei/section) were positive with a late G_2-M phase marker, pH3-S10, at 7 d.p.i., and judging from the morphology of their nuclei, these cells appeared to be at late G_2-phase (Fig. 2*C*). These data suggested that many CMs reentered the cell cycle, but the cycle was arrested before M-phase.

Expression and Activities of Cyclin-CDK Complexes after Cyclin D1 Induction—Induction of cyclin D1 suggested cell cycle reentry in many CMs. Next, we examined the expression and activities of main cyclin-CDK complexes.

Western blot analysis showed that expression of exogenous cyclin D1 was detected from 3 d.p.i., after which the protein level remained constant thereafter (Fig. 3*A*). The expression levels of other main cyclins and CDKs were very low or at the background levels in control mice (see 0 d.p.i. in Fig. 3*A*) (9). However, these protein levels increased markedly by induction of cyclin D1 and showed a peak at 5 or 7 d.p.i. In addition, these patterns were similar to those of the mRNAs (Fig. 3*B*). These results showed that the expression of main cyclins and CDKs was induced by cyclin D1 induction; however, the levels decreased after 7 d.p.i.

We also examined the expression of proteins related to DNA replication (Cdt1, Geminin, Mcm3, and Mcm4; Fig. 3, *C* and *D*). These protein levels were increased by administration of Tam and showed a peak at 5 or 7 d.p.i., although the increase in Cdt1 was only slight. Expression of Cip/Kip family proteins was also examined (Fig. 3*E*). $p21^{Cip1}$ levels increased by induction of

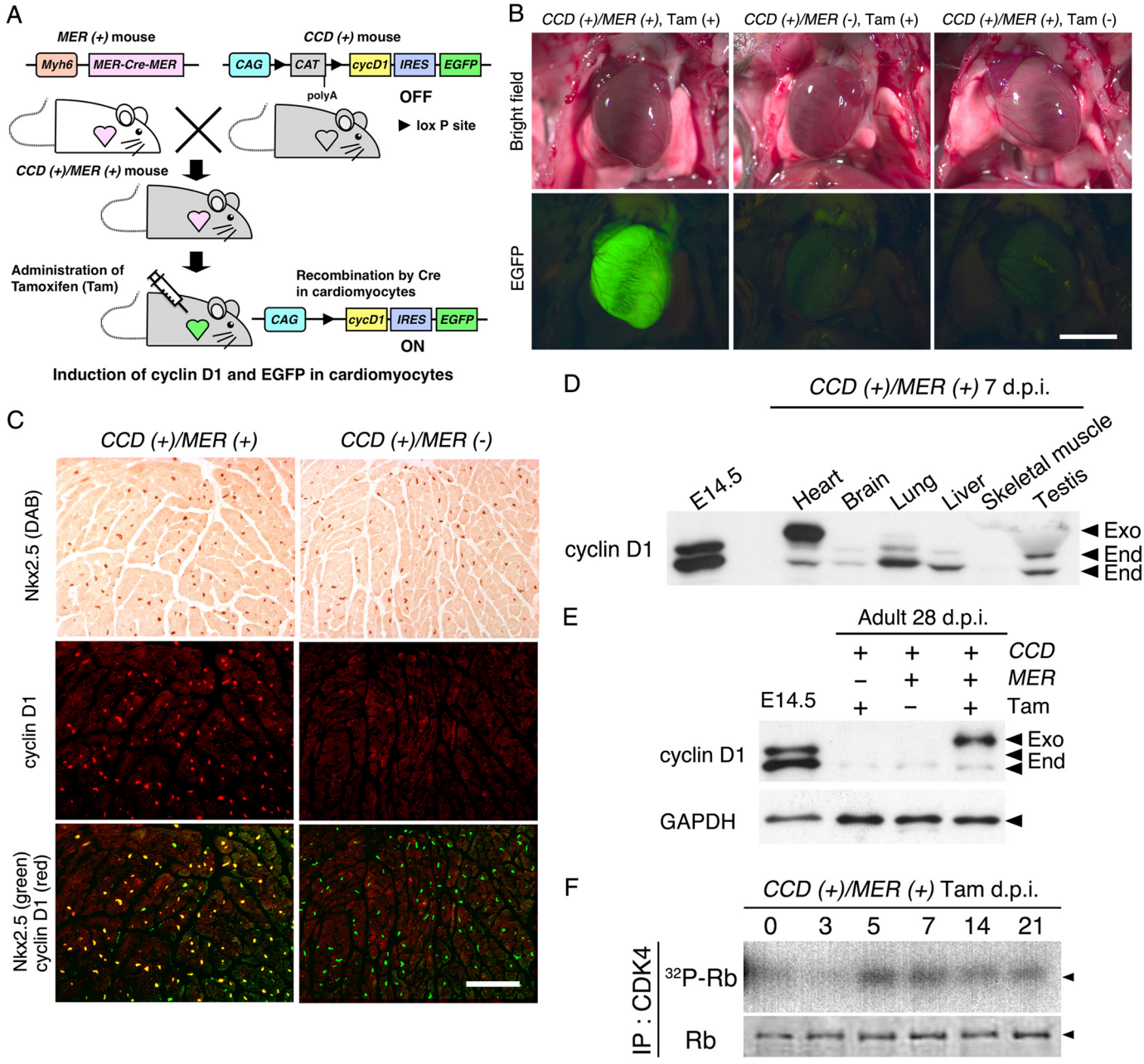

FIGURE 1. **CM-specific induction of cyclin D1 expression in adult *CCD*(+)/*MER* (+) mouse by Tam administration.** *A*, the constructs of transgenes are shown. *CCD* (+)/*MER* (+) mice were generated by intercrossing between *CCD* (+) and *MER* (+) mice. MER-Cre-MER localizes from cytoplasm to nuclei in CMs by administration of Tam and excludes the sequences containing the *CAT* gene with poly(A) signal between *loxP* sites only in differentiated CMs, resulting in CM-specific induction of cyclin D1 and EGFP expression. *B*, the bright field (*upper panels*) and EGFP fluorescence (*lower panels*) images of the hearts of cyclin D1-induced (*CCD* (+)/*MER* (+), Tam (+)) and control (*CCD* (+)/*MER* (−), Tam (+), and *CCD* (+)/*MER* (+), Tam (−)) mice at 7 d.p.i. are shown. Tam (+) and Tam (−) indicate mice administered Tam and only vehicle, respectively. These images were photographed immediately after thoracotomy. *Scale bar*, 5 mm. *C*, cardiac sections of mice at 7 d.p.i. of Tam were immunostained with an antibody against a CM marker, Nkx2.5, using a peroxidase-labeled antibody method (*DAB*, *upper panels*), and then the same sections were stained with an antibody against cyclin D1 (*red*) using an immunofluorescence method (*middle panels*). These images were merged (*lower panels*), and double-positive CM nuclei with Nkx2.5 (pseudo-color, *green*) and exogenous cyclin D1 (*red*) are visualized in *yellow*. These double-positive cells were also positive for sarcomeric actin. *Scale bar*, 100 μm. *D*, tissue specificity of exogenous cyclin D1 expression. A *CCD* (+)/*MER* (+) adult mouse was administered Tam, and equal amounts of extracts from the indicated tissues at 7 d.p.i. were analyzed by Western blot analysis. Whole embryos at E14.5 were used as a positive control. *Arrowheads* show the positions of positive signals. *Exo* and *End* indicate exogenous and endogenous cyclin D1, respectively. *E*, genotype and Tam specificity of exogenous cyclin D1 induction. Equal amounts of extracts from the cardiac ventricles of the indicated mice at 28 d.p.i. were analyzed by Western blot analysis. Whole embryos at E14.5 were used as a positive control. GAPDH was used as an endogenous control. *F*, CDK4 activation by cyclin D1 induction. Equal amounts of extracts from the cardiac ventricles of *CCD* (+)/*MER* (+) adult mice administered Tam were immunoprecipitated with an antibody against CDK4 at indicated d.p.i. The immunoprecipitates (*IP*) were analyzed with an *in vitro* kinase assay using Rb as a substrate. ^{32}P-Labeled Rb (*upper panel*), autoradiograph for phosphorylated Rb. Rb (*lower panel*), Coomassie Brilliant Blue staining images of Rb. Arrowheads show the positions of positive signals.

cyclin D1, although those of $p27^{Kip1}$ did not show apparent changes. $p57^{Kip2}$ was not detected in all adult heart samples. The result was consistent with that of a previous study (23).

We next examined the activities of cyclin-CDK complexes with *in vitro* kinase assay after immunoprecipitation using antibodies against cyclin E, A, or B1 (Fig. 4, *A* and *B*). The patterns

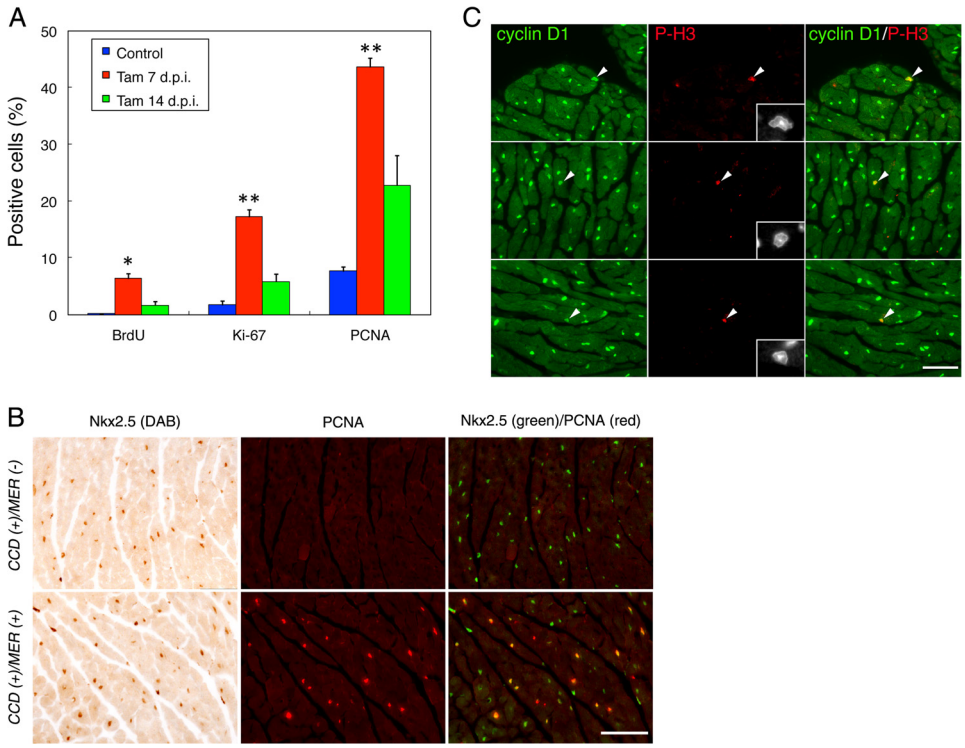

FIGURE 2. **Increase in proliferation marker-positive CMs by cyclin D1 induction.** *A*, percentages of positive cells for proliferation markers among CMs. Cardiac sections of control adult mice (single hemizygote mice at 7 d.p.i. of Tam) and *CCD* (+)/*MER* (+) adult mice at 7 and 14 d.p.i. of Tam were immunostained with antibodies against proliferation markers and a CM marker, Nkx2.5. Percentages of double-positive cells among Nkx2.5 positive cells in the ventricles were calculated and are shown as the means ± S.E. $n = 3$. *, $p < 0.05$; **, $p < 0.01$ *versus* control mice (Tukey's test after obtaining a significant difference with one-way analysis of variance). These double-positive cells were also positive for sarcomeric actin. *B*, cardiac sections of the indicated adult mice at 7 d.p.i. of Tam were co-immunostained with antibodies against PCNA (*red*) and Nkx2.5. The merged images in the left ventricle are shown. The same methods as described in Fig. 1*C* were used. Double-positive CM nuclei with Nkx2.5 (pseudo-color, *green*) and PCNA (*red*) are visualized in *yellow*. *Scale bar*, 100 μm. *C*, cardiac sections of *CCD* (+)/*MER* (+) mice at 7 d.p.i. of Tam were coimmunostained with antibodies against cyclin D1 and pH3-S10. *Arrowheads* show very rare double-positive cardiomyocyte nuclei with cyclin D1 (*green*, exogenous expression) and pH3-S10 (*red*) in three independent images in the left ventricles. *Insets* show the high power views of the pH3-S10-positive nuclei stained with DAPI. These nuclei appear to be at late G_2-phase because nuclear membrane and nucleoli, but not any chromosome condensation, can be seen. Because signals for Nkx2.5 in phospho-H3-S10 positive nuclei are very weak, cyclin D1 was used as a marker for cardiomyocytes. *Scale bar*, 50 μm.

of the immunoprecipitated cyclins and CDKs were similar to those in Fig. 3*A* (Fig. 4*A*). However, the kinase activity of cyclin A-CDK was low, and that of cyclin B1-CDK was extremely low at 5 and 7 d.p.i., although that of cyclin E-CDK was high (Fig. 4, *A* and *B*).

The cyclin-CDK1 complex is the master regulator of mitosis, and inhibition of its activation induced G_2 arrest or endoreplication in various species and cells (24, 25). Because the dephosphorylation of both Thr-14 and Tyr-15 is required for the activation of CDK1 and entry into M-phase (26), we examined the phosphorylation pattern in the hearts of *CCD* (+)/*MER* (+) mice. Mammalian CDK1 that co-immunoprecipitated with cyclin B1 was detected as three different bands on SDS-PAGE. The upper, intermediate, and lower bands represent CDK1 of double-phosphorylated (Thr-14 and Tyr-15), single-phosphorylated (Thr-14 or Tyr-15), and unphosphorylated forms, respectively (27, 28). We found that the slowest-migrating form of CDK1 (the upper band) was detected as the major band at 5 and 7 d.p.i., which was positive for a phospho-Tyr-15 antibody. In contrast, the intermediate and lower bands were not detected and very faint, respectively (Fig. 4, *A* and *C*). On the other hand, the lower band of CDK1 in whole embryos at E10.5 was apparent, which is consistent with high CDK1 activity (Fig. 4, *A* and *C*). These results indicated that the failed dephosphorylation of Thr-14 and Tyr-15 resulted in inactivation of CDK1 in the CMs of cyclin D1-induced mice.

Thr-14 and Tyr-15 of CDK1 are dephosphorylated by Cdc25. We also found that mRNA expression of *Cdc25c*, one of the *Cdc25* subtypes, increased significantly at 7 d.p.i., but those of *-b* or *-c* were not increased and were maintained at low levels after Tam treatment (Fig. 4*D*; *Cdc25a*, *-b*, and *-c*, 1.26-, 1.03-, and 24.0-fold of the control, respectively). Cdc25a and -b proteins were not detected in any adult heart samples (Fig. 4*E*). We could not find any anti-Cdc25c antibodies that can detect mouse Cdc25c. Deficiency in increases of *Cdc25a* and *-b* expression is important, because all *Cdc25* subtypes show high expression in embryonic and postnatal stages around P5 when mitotic activities are high.[5] Moreover, knockdown of both Cdc25a and -b inhibits M-phase entry and reduced dephosphorylation and the activity of CDK1 in cultured cells (29). These data are similar to our results (Fig. 4). In addition, conditional knock-out (KO) experiments of single, double, and triple *Cdc25* subtypes revealed that only triple and double (*Cdc25a* and *-b*) KO mice show robust phenotypes in intestinal epithelial cells, such as the inhibition of mitosis (30, 31). These reports indi-

[5] S. Ogawa, M. Kubota, and T. Takeuchi, unpublished data.

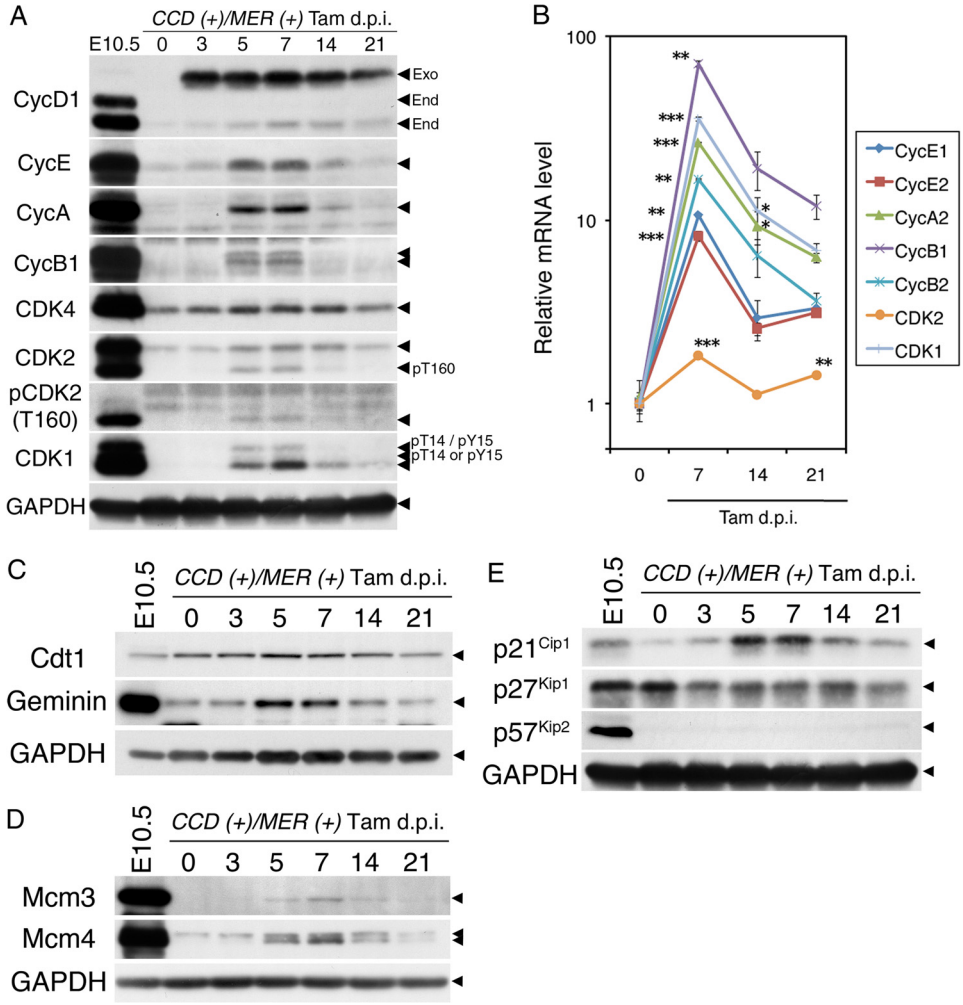

FIGURE 3. **Expression patterns of cell cycle regulators in hearts of adult *CCD* (+)/*MER* (+) mice after administration of Tam.** *A* and *C–E*, protein expression in the cardiac ventricles was examined by Western blot analysis (*A* and *E*, each lane, 50 μg of protein; *C*, 15 μg of protein; *D*, 20 μg of protein). Extracts from whole embryos at E10.5 were used as a positive control. *Arrowheads* show the positions of positive signals. *Exo* and *End* represent exogenous and endogenous cyclin D1, respectively. The well known band shifts by phosphorylation are indicated in CDK2 or CDK1. GAPDH was used as an endogenous control. *E*, GAPDH controls are same as those in *A* because the same membrane was used. *B*, real-time RT-PCR analyses were performed in duplicate using cDNA from the cardiac ventricles of *CCD* (+)/*MER* (+) adult mice at indicated d.p.i. The relative mRNA levels are presented as the mean ± S.E. *, $p < 0.05$; **, $p < 0.01$; ***, $p < 0.005$ *versus* 0 d.p.i. (Tukey's multiple comparison test after obtaining a significant difference with one-way analysis of variance). The *vertical axis* is shown as a logarithmic scale.

cated that both Cdc25a and -b are necessary for M-phase entry through dephosphorylation of CDK1. Thus, a deficiency in increases of *Cdc25a* and *-b* expression can explain the mechanism that inhibits activation of CDK1.

It is known that the activation of ATM/ATR pathways is involved in the inhibition of CDK1 activation in the G_2 checkpoint (32, 33). Phosphorylation of ATM/ATR targets (histone H2AX, Chk1, and p53) are tightly associated with the activation of ATM/ATR pathways (34–37). Therefore, we investigated the expression and phosphorylation of these ATM/ATR targets after induction of cyclin D1. Although H2AX and Chk1 were detected, the phosphorylated forms (γ-H2AX and pChk1-S345) were not observed in the cardiac ventricles of control or cyclin D1-induced mice (Fig. 5, *A* and *B*). Protein expression of p53 was not detected in the cardiac ventricles of either mouse (Fig. 5*C*). The absence of p53 in the ventricles is consistent with that of a previous report (38). These results indicated that inhibition of CDK1 dephosphorylation, observed in cyclin D1-induced mice, was independent of ATM/ATR pathways.

Reentry by >40% of CMs to the Cell Cycle by Cyclin D1 Induction—Remarkable increases in proliferation markers (Fig. 2*A*) and in the expression and activities of cyclin-CDK complexes (Fig. 3) strongly suggested that many adult CMs reentered the cell cycle by induction of cyclin D1. To study how many adult CMs reentered the cell cycle and to determine to what phase the cell cycle of these CMs proceeded, we next analyzed the cell cycle distribution patterns in *CCD* (+)/*MER* (+) CMs after Tam administration. We measured the DNA content per nucleus of a single CM dissociated from the ventricles on slide glasses, because FACS analysis can neither measure the DNA content in each nucleus in binucleated CMs nor distinguish between mono- and binucleated CMs. The method for mouse cardiomyocytes has been established (9). Nuclei with 2C, 2C-4C, and 4C were regarded as those in G_1-, S-, and G_2/M-phase, respectively. In addition, to monitor the cell cycle progression of adult CMs after induction of cyclin D1, we simultaneously performed EdU pulse-chase experiments.

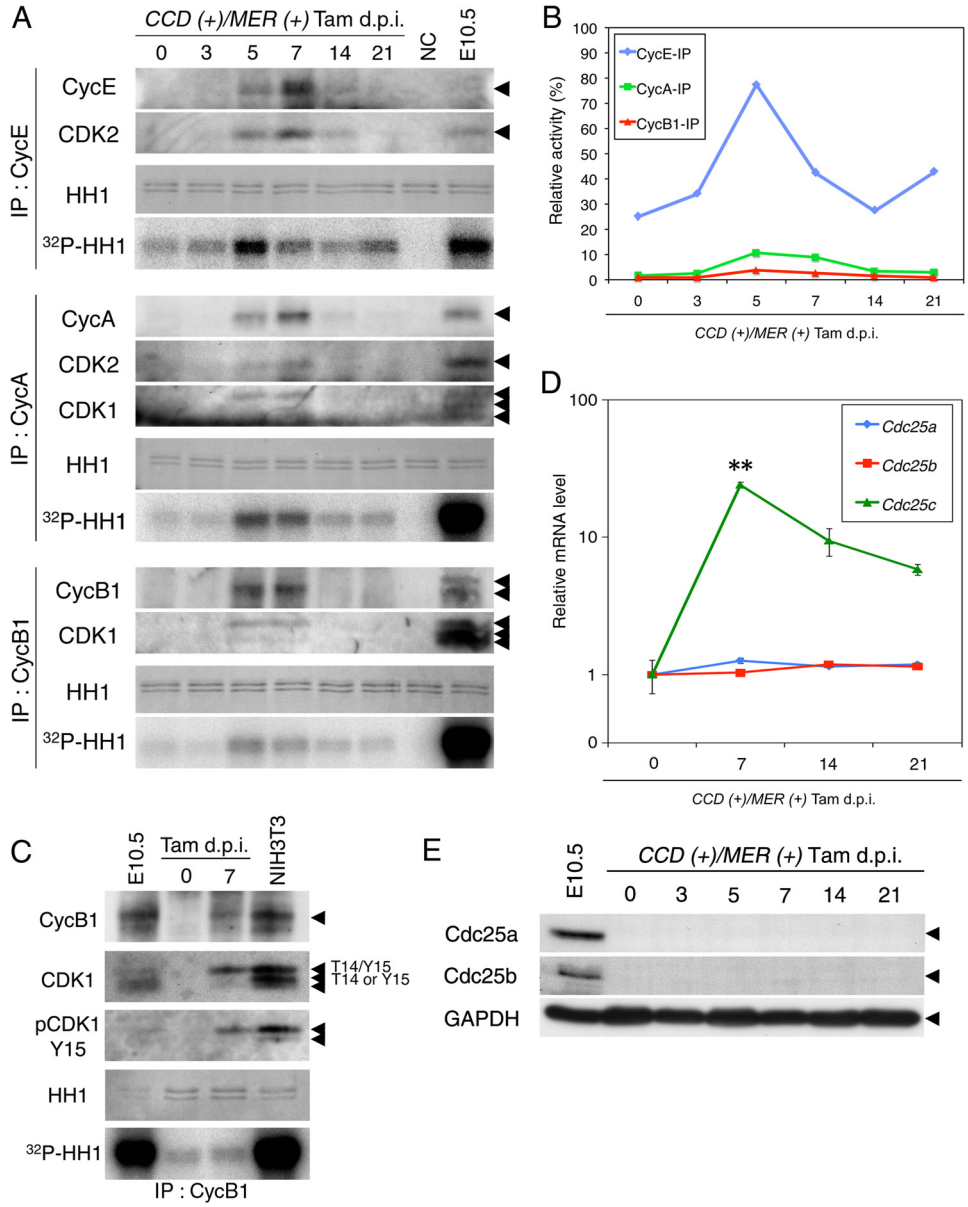

FIGURE 4. **Inhibition of cyclin B1-CDK1 activation in adult hearts after induction of cyclin D1.** *A*, CDKs bound to cyclin E (CycE-IP), cyclin A (CycA-IP), and cyclin B1 (CycB1-IP) were immunoprecipitated (*IP*) with corresponding cyclin antibodies from the cardiac ventricles of *CCD* (+)/*MER* (+) adult mice at indicated d.p.i. of Tam. Protein patterns of cyclin-CDK complexes were analyzed by Western blot analysis. *Arrowheads* show the positions of positive signals and phosphorylation forms in CDK1. CDK activities of these complexes were analyzed with an *in vitro* kinase assay using histone H1 as a substrate. Coomassie Brilliant Blue staining image of histone H1 and autoradiograph indicating phosphorylated histone H1 are shown as HH1 and ^{32}P-labeled HH1, respectively. Whole embryos at E10.5 were used as a reference for CDK activities. Due to the strong activities, the protein contents of these references used were one-tenth those in *CCD* (+)/*MER* (+) mice. *NC*, negative controls using no immunoprecipitates for *in vitro* kinase assay. *B*, activities of CDKs in *A* are shown as percentages of relative levels to whole embryos at E10.5. *C*, phosphorylation patterns of CDK1 immunoprecipitated with an anti-cyclin B1 antibody in the ventricles of *CCD* (+)/*MER* (+) adult mice at indicated d.p.i. of Tam were analyzed by Western blot analysis. Whole embryos at E10.5 and growing NIH3T3 cells were used as references exhibiting three phosphorylation forms. Due to the strong signals, the protein contents of these references used were one-tenth of those in *CCD* (+)/*MER* (+) mice. pCDK1-Tyr-15, antibody for phospho-CDK1-Tyr15. *Arrowheads* show the positions of positive signals and phosphorylation forms in CDK1. The activities of cyclin B1-CDK1 complexes were analyzed and are shown as *A*. *D*, real-time RT-PCR analyses were performed in duplicate using cDNA from the cardiac ventricles of *CCD* (+)/*MER* (+) adult mice at the indicated d.p.i. The relative mRNA levels of *Cdc25a-c* are presented as the mean ± S.E. **, $p < 0.01$ *versus* 0 d.p.i. (Tukey's multiple comparison test after obtaining a significant difference with one-way analysis of variance). The *vertical axis* is shown as a logarithmic scale. *E*, Cdc25a and -b protein expression in the cardiac ventricles was examined by Western blot analysis (each lane, 20 μg of protein). Extracts from whole embryos at E10.5 were used as a positive control. *Arrowheads* show the positions of positive signals. GAPDH was used as an endogenous control.

The induction of cyclin D1 caused prominent cell cycle entry in adult CMs. DNA content of the majority of nuclei (91.5%) was 2C in total CMs of control mice, whereas 4C nuclei were rare (3.9%) (Fig. 6, *A* and *B*). After induction of cyclin D1, 2C nuclei gradually decreased, whereas 4C nuclei increased (Fig. 6, *A*–*C*). The final percentages of 2C and 4C were 44.2 and 30.8%, respectively (Fig. 6*B*), showing that >40% of total CM nuclei entered the cell cycle (91.5 − 44.2 = 46.3%). These percentages of binucleated cells were almost the same as those of total CMs (Fig. 6, *A* and *B*). The cell cycle progression of mononucleated CMs was more prominent. The percentages of 2C and 4C in mononucleated CMs of control were 72.8 and 18%, respectively

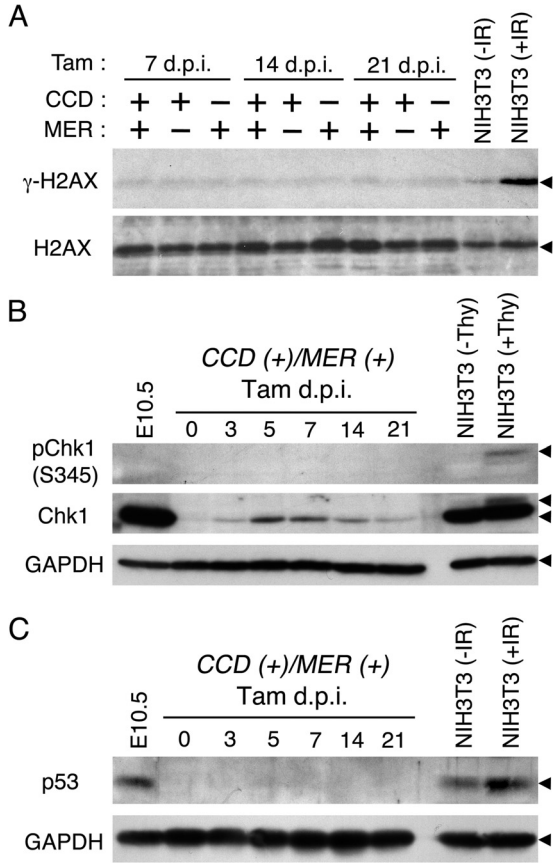

FIGURE 5. **Phosphorylated forms of histone H2AX and Chk1 and expression of p53 are not detected after induction of cyclin D1.** Phosphorylated histone H2AX (γ-*H2AX*), histone H2AX (*H2AX*) (*A*), phosphorylated Chk1 (*pChk1-S345*), Chk1 (*B*), and p53 (*C*) were analyzed by Western blot analysis using extracts from the cardiac ventricles of *CCD* (+)/*MER* (+) adult mice or other genotyped mice at indicated d.p.i. of Tam. NIH3T3 cells were used as positive (+*IR* and +*Thy*) and negative controls (−*IR* and −*Thy*) for phosphorylation. +*IR*, irradiated at 10-gray dose; −*IR*, no irradiation; +*Thy*, treated with 2 mM thymidine for 20 h; −*Thy*, no treatment with thymidine. Whole embryos at E10.5 were also used as a positive control for Chk1 and p53.

(Fig. 6, *A* and *B*). Mononucleated CMs with 2C were decreased markedly by induction of cyclin D1. On the other hand, cells with 4C or >4C were increased (Fig. 6, *A–C*). The final percentages in 2C, 4C, and >4C CMs were 8.5, 36.8, and 48.1%, respectively (Fig. 6*B*), showing that >60% of mononucleated CMs entered the cell cycle (at least, 72.8 − 8.5 = 64.3%), and many of these cells entered endoreplication. The effects due to Tam are excluded because no apparent changes were observed in a *CCD* (+)/*MER*(−) mouse at 14 d.p.i. of Tam (Fig. 6*Ab*).

We also compared the percentages in 2C, 2C-4C, 4C, and >4C CMs of multiple mice at 14 d.p.i., and the changes in 2C and 4C in both bi- and mononucleated CMs and in >4C CMs of mononucleated CMs were significant (Fig. 6*D*). These data also showed that ~40 and 60% of bi- and mononucleated CMs entered the cell cycle at the stage, respectively (control 2C (%) − *CCD* (+)/*MER*(+) 2C (%): binucleated CMs, 90.1–51.6 = 38.5%; mononucleated CMs, 72.6–12.9 = 59.7%).

EdU was injected at 5 d.p.i. or at both 5 and 7 d.p.i. EdU-positive nuclei of the total and binucleated CMs were mainly detected in the 4C population (Fig. 6*Aa*). EdU-positive mononucleated CMs were found first in the 4C population at 7 d.p.i. Subsequently, 8C CMs were detected at later time points (Fig. 6*Aa*), indicating that these CMs entered endoreplication by skipping M-phase. No EdU-positive 2C nuclei was observed in either mono- or binucleated CMs, indicating that these cells could not complete karyokinesis or cytokinesis (Fig. 6*Aa*). These results were consistent with the findings that mitotic CMs were not observed (Fig. 2*C*) and that the kinase activity of cyclin B1-CDK was extremely low (Fig. 4).

These data showed that >40% of CMs reentered the cell cycle. The cell cycle of almost all of these binucleated CMs was arrested before M-phase, and many mononucleated CMs entered endoreplication, suggesting inhibition of M-phase entry in both CMs.

Increase in $p21^{Cip1}$ Is Not Essential for Inhibition of the M-phase Entry—Finally, we examined whether the increase in $p21^{Cip1}$ level (Fig. 3*E*) inhibited M-phase entry. We produced double transgenic and $p21^{Cip1}$ knock-out mice (*CCD* (+)/*MER* (+); $p21^{Cip1-/-}$) by crossing, and then Tam was administered. The cell cycle distribution patterns of these mice and control KO mice (*CCD* (−)/*MER*(−); $p21^{Cip1-/-}$) were examined. The patterns of the control mice showed abnormalities (increases of nuclei in 4C in both mono- and binucleated CMs and 8C in mononucleated CMs) (Fig. 7*A*, *left*) as compared with wild type control mice (Fig. 6*Aa*, *Control*). However, the abnormalities would result from those that occurred during postnatal stages, because CMs in $p21^{Cip1-/-}$ mice already showed the same phenotypes at P14 (23) and no EdU positive CMs were detected in the adult *CCD* (−)/*MER* (−); $p21^{Cip1-/-}$ mouse (Fig. 7*A*, *left*). Effects of cyclin D1 induction were observed in the *CCD* (+)/*MER*(+); $p21^{Cip1-/-}$ mouse, as 2C nuclei decreased and those of 4C (both mono- and binucleated CMs) and 8C (mononucleated CMs) increased compared with the *CCD* (−)/*MER* (−); $p21^{Cip1-/-}$ mouse (Fig. 7, *A* and *B*). These features were similar to those of *CCD* (+)/*MER* (+); $p21^{Cip1+/+}$ mice (Fig. 6*D*). If CMs enter the M-phase, increases in EdU-positive 2C nuclei and/or tri- or tetranucleated CMs are expected. However, most of the EdU-positive nuclei were not in 2C in both mono- and binucleated CMs. Only two 2C nuclei were observed in a binucleated CM. In addition, the percentages of tri- and tetranucleated CMs did not increase in the *CCD* (+)/*MER* (+); $p21^{Cip1-/-}$ mouse at 14 d.p.i. of Tam (Fig. 7*C*). Although the percentage of binucleated CMs increased slightly, a similar increase was observed in the *CCD* (+)/*MER* (+); $p21^{Cip1+/+}$ mice (Fig. 6*Bb*). Therefore, we concluded that an increase in $p21^{Cip1}$ is not essential for the inhibition of M-phase entry.

DISCUSSION

The expression of cyclin D1 as well as other D-type cyclins and main cyclins decrease to very low levels after P14 when binucleation is almost completed. The silent state of cyclin D1 is maintained for life (7, 9). In the present experiments we showed that induction of cyclin D1 caused an increase in expression of main cyclins and CDKs and cell cycle reentry in >40% of CMs (Figs. 2, 3, 6, and 7). These results show that silencing the cyclin D1 expression is necessary for the maintenance of the cell cycle exit in many CMs. D-type cyclins (D1, D2, and D3) have critical and redundant functions in cardiomyocyte proliferation because triple, but not single or double knock-out, mice showed phenotypes in the cardiomyocyte

proliferation (39). These results suggest that silencing the expression of other D-type cyclins (D2 and D3) is also necessary for the maintenance of the cell cycle exit in CMs. After cell cycle reentry, the cell cycle of CMs was arrested in 4C (binucleated cells) and 4C or 8C (mononucleated cells) (Fig. 6). These results suggest two possibilities.

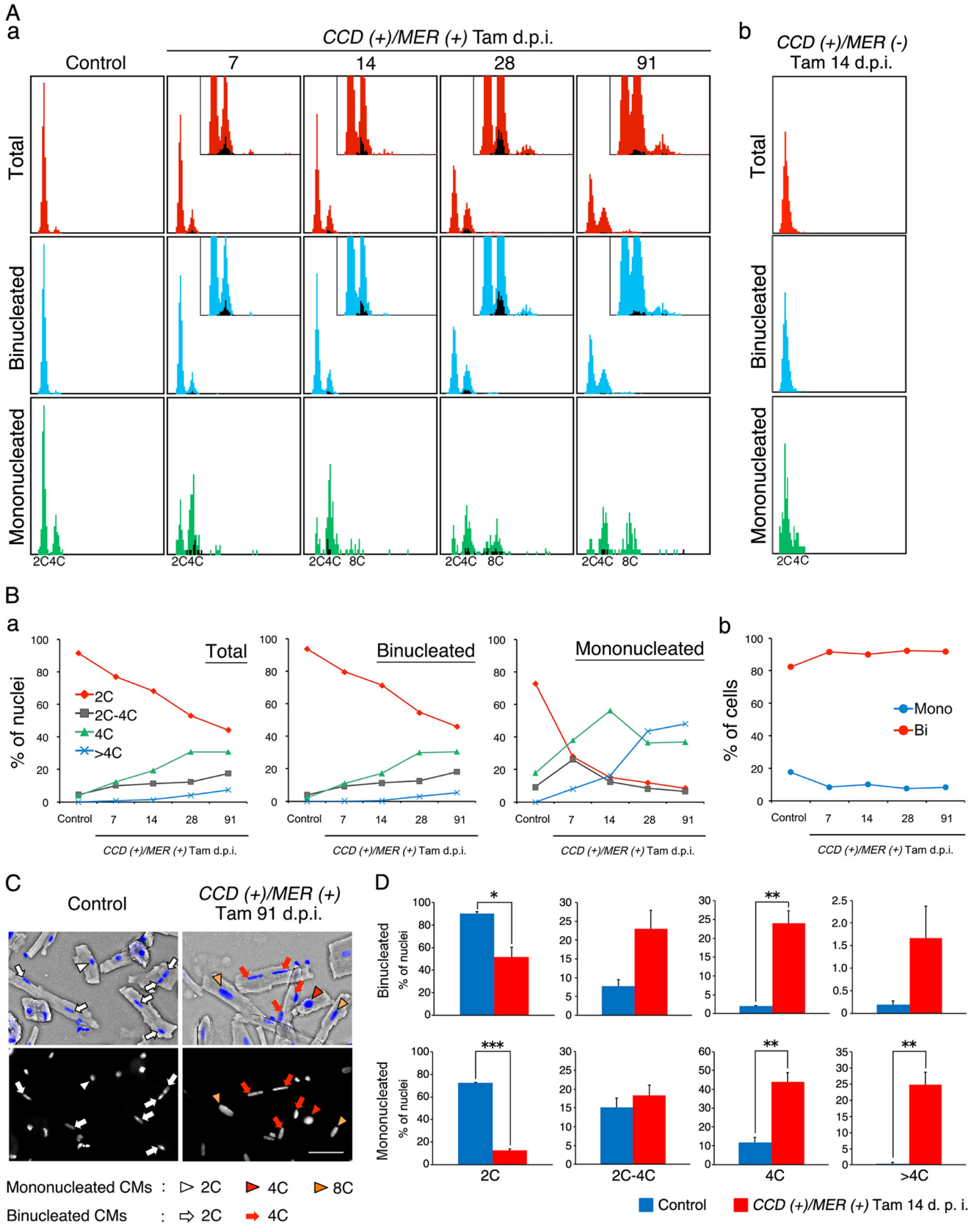

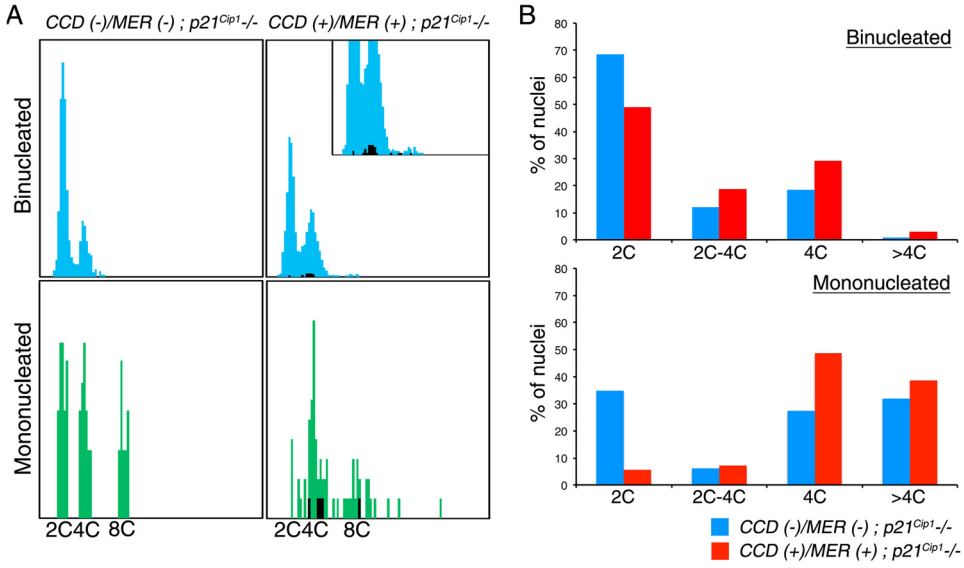

C

	CCD (-)/MER (-) ; $p21^{Cip1-/-}$	CCD (+)/MER (+) ; $p21^{Cip1-/-}$
Mononucleated	6.4%	4.0%
Binucleated	88.0%	92.4%
Tri- / tetranucleated	5.3%	3.6%
No. of analyzed CMs	1042	1074

FIGURE 7. **$p21^{Cip1}$ is not essential for inhibition of the M-phase entry.** *A*, the histograms show the number of nuclei with various DNA contents for bi- (*upper*) and mononucleated (*lower*) CMs in *CCD* (−)/*MER* (−); $p21^{Cip1-/-}$ and *CCD* (+)/*MER* (+); $p21^{Cip1-/-}$ mice at 14 d.p.i. of Tam. EdU-positive nuclei are shown in *black*. *Insets* show the magnified images. EdU was injected at both 5 and 7 d.p.i. No EdU positive CMs were detected in the *CCD* (−)/*MER* (−); $p21^{Cip1-/-}$ mouse. *B*, percentages of 2C, 2C-4C, 4C and >4C populations in bi- and mononucleated CMs of mice in *A*. *C*, percentages of mono-, bi-, and tri-/tetranucleated CMs of mice in *A*.

One is that the G_2 checkpoint was induced by negative effects due to cyclin D1 induction, such as DNA damage, incomplete DNA replication, or prolonged expression of cyclin D1, and the checkpoint prevented CMs from entering mitosis. The G_2 checkpoint is regulated by ATM/ATR pathways, including $p21^{Cip1}$ and Cdc25 (40, 41). However, no signs indicating activation of ATM/ATR or DNA damage were detected in the hearts of control or cyclin D1-induced mice (before and after cell cycle reentry, Fig. 5). In addition, the DNA content of many mononucleated CMs in cyclin D1-induced mice increased to 8C from 4C (Fig. 6), suggesting completion of DNA replication.

Regarding $p21^{Cip1}$, the protein level increased after cyclin D1 induction (Fig. 3*E*). However, the upstream protein, p53 in ATM/ATR pathways (40, 41) was not detected in any adult hearts (Fig. 5*C*). Moreover, CMs of $p21^{Cip1}$ knock-out mice, in which cyclin D1 was induced, still did not exhibit robust M-phase entry (Fig. 7), indicating that an increase in $p21^{Cip1}$ is not essential for inhibition of the M-phase entry. $p21^{Cip1}$ has positive functions for cell cycle progression as well as negative functions (11), suggesting that the increase was related to cell cycle progression. In fact, $p21^{Cip1}$ is highly expressed in mouse embryonic hearts when the proliferation activities are high (23). Regarding Cdc25, the expression of *Cdc25a* and *-b* did not increase after cyclin D1 induction (Fig. 4, *C* and *D*). In ATM/ATR pathways, *Cdc25c* among *Cdc25* subtypes is repressed by p53 (40, 41). These facts cannot explain the deficiency in increases of *Cdc25a* and *-b*. These results suggest that an increase in $p21^{Cip1}$ and deficiency in increases of *Cdc25a* and *-b* are not related to ATM/ATR pathways.

Another possibility is that CMs have a natural system independent of the negative effects due to cyclin D1 induction, and the system also prevents CMs from entering mitosis after cell cycle reentry. To prove the possibility, we need to demonstrate the same phenotypes in other mouse systems that are independent of the negative effects of cyclin D1 induction and show cell cycle reentry. We have observed similar phenotypes to cyclin D1-induced mice; increases in 4C (both mono- and binucleated CMs) and 8C (mononucleated CMs) populations, in $p21^{Cip1}$ and $p27^{Kip1}$ knock-out mice (23).

From the discussion above, the second possibility, which is that CMs have a natural system inhibiting M-phase entry, is

FIGURE 6. **Reentry by >40% of CMs to the cell cycle by cyclin D1 induction.** *Aa*, the histograms showed the number of nuclei with various DNA content of total (*upper*), bi- (*middle*), and mononucleated (*lower*) CMs in adult control mice (wild type mice at 7 d.p.i. of Tam) and *CCD* (+)/*MER* (+) mice at 7, 14, 28, and 91 d.p.i. of Tam. EdU-positive nuclei are shown in *black*. Insets show the magnified images. EdU was injected into *CCD* (+)/*MER* (+) mice at 5 d.p.i. for analysis at 7 d.p.i. or at both 5 and 7 d.p.i. for analysis on other days. *b*, a negative control using *CCD* (+)/*MER* (−) mice at 14 d.p.i. of Tam. *Ba*, percentages of nuclei with 2C, 2C-4C, 4C, and >4C in the cell cycle distribution patterns of total and mono- and binucleated CMs in indicated mice in *A*. *b*, the percentages of mono- and binucleated CMs in the indicated mice in *A*. *C*, examples of single CMs dissociated from ventricles of control and *CCD* (+)/*MER* (+) mice at 91 d.p.i. of Tam. Images stained with DAPI (*lower panels*) were merged with bright field images (*upper panels*). DAPI signals are shown in *blue*. *Arrowheads* and *arrows* represent various DNA contents (2C, 4C, or 8C) in nuclei of mono- and binucleated CMs, which were determined by measurement of DAPI fluorescence intensity. *Scale bar*, 50 μm. *D*, percentages of 2C, 2C-4C, 4C, and >4C populations in bi- and mononucleated CMs in adult control mice (single hemizygote mice) and *CCD* (+)/*MER* (+) mice at 14 d.p.i. of Tam (mean ± S.E., $n = 3$). *, $p < 0.05$; **, $p < 0.01$; ***, $p < 0.005$ *versus* control mice (Student's *t* test).

more likely. The system would function to maintain cell cycle exit as well as silencing the cyclin D1 expression. As the mechanism of the system, deficiency in increases of *Cdc25a* and *-b* expression (Fig. 4, *D* and *E*) can explain the inhibition of CDK1 activation (Fig. 4, *A–C*), because both Cdc25a and -b are necessary for M-phase entry (29–31). If this is the case, the core of the system inhibiting M-phase entry is the silencing of the expression of *Cdc25a* and *-b* and its maintenance.

Previous transgenic studies have shown the effects of exogenous D-type cyclins driven by the *Myh6* promoter in CMs; however, these results are markedly different from our data (42, 43). Reentry to the cell cycle by many adult CMs, which was observed in the present study (>40%, PCNA staining and cell cycle distribution patterns; Figs. 2 and 6), was not reported in these studies (at most, 0.3% incorporation of tritiated thymidine in intact mice) (42, 43). The most critical difference in methods is the developmental stages when exogenous D-type cyclins were expressed. D-type cyclins were expressed continuously from embryos to adults in the previous studies, because the *Myh6* promoter works from early embryonic stages (18, 44). By contrast, we expressed cyclin D1 only at adult stages using an inducible Cre-loxP system (Fig. 1). The strong effects of cyclin D1 induction on cell cycle progression or main cell cycle regulators were transient (Figs. 2–4). Therefore, we speculate that the strong effects had transiently occurred only at embryonic or postnatal but not adult stages in the previous studies. In fact, the increase in expression of main cell cycle regulators was not high at adult stages. Especially, CDK1 expression was not detected (42, 43).

In the present study we analyzed the cell cycle distribution patterns of CMs in cyclin D1-induced mice by measurement of DNA content per nucleus and EdU pulse-chase experiments. The combined method can show completion of karyokinesis and cytokinesis by detecting an EdU-positive 2C nucleus in CMs. Thus, this method is a powerful tool with which analyze completion of mitosis. However, we could identify neither karyokinesis nor cytokinesis in the CMs of cyclin D1-induced adult mice, because no EdU-positive 2C nuclei were observed using this method. In addition, no pH3-S10 positive cells showed mitotic figures (Fig. 2*C*). These data indicated that mitosis of CMs, if any, would occur very rarely in cyclin D1-induced mice. Recent studies reported that a small number of CMs can complete mitosis at postnatal or adult stages (4, 5, 45, 46). The evaluation of karyokinesis and cytokinesis in some studies mainly depends on immunostaining against pH3-S10 or Aurora B in cardiac sections. However, it is impossible to conclude the completion of karyokinesis or cytokinesis only by these stainings. Evaluation of these results with methods such as ours will be more reliable.

The following two issues are important when considering further molecular mechanisms of cell cycle exit of CMs. First, what factors are required for maintenance of the silent state of cyclin D1? We speculate that epigenetic regulation maintains silencing of these genes because mRNA levels of these genes are down-regulated (data not shown). Second, what mechanisms are involved in the inhibition of cyclin B1-CDK activation in postnatal CMs? Deficiency in increases of *Cdc25a* and *-b* is more likely (Fig. 4, *D* and *E*). This needs to be proven, and how the silent state is maintained in an ATM/ATR independent manner should also be examined.

Elucidation of these issues will provide new insights to facilitate the proliferation of the CMs and will contribute to regenerative therapy by the proliferation of pre-existing CMs. It is very interesting that CMs have multiple systems for cell cycle exit (at least three systems; silencing the cyclin D1 expression, inhibition of M-phase entry, and a system inhibiting cytokinesis) in postnatal and adult mammals, which is distinct from non-mammalian model animals, which can regenerate their hearts at adult stages, such as zebrafish and newts (47, 48). Why do mammals have multiple inhibitory systems? We speculate that the robust cell cycle exit is necessary for the homeostasis of mammalian cardiac functions, and the multiple systems act as a backup mechanism to maintain the cell cycle exit robustly in postnatal and adult CMs. This could be examined and verified by canceling all inhibitory systems. If this is the case, careful manipulation of the reset of cell cycle exit is required for regenerative therapy. Future studies regarding cell cycle exit of CMs will be able to clarify the possibility of cardiac regeneration in mammals, significance of cell cycle exit in cardiac functions, and the property that determines the difference in CM proliferation and cardiac regeneration between mammalian and non-mammalian model animals.

Acknowledgments—We thank the following for kind gifts; Dr. Philip Leder (p21^{Cip1} KO mice), Dr. Yumiko Saga (pBSKISecI CAG-CAT-Poly(A)), and Drs. Hideo Nishitani (University of Hyogo, Ako) and Dr. Keiko Nakayama (Tohoku University, Sendai) (antibodies). We thank Dr. Toru Nakano (Osaka University, Suita) for critical reading of the manuscript. We also thank Mizuyo Kojima, Kuniko Nakajima, Rika Suzuki-Migishima, Toshiaki Hino (Mitsubishi Kagaku Institute of Life Sciences, Machida), and Satomi Ikuta (Tottori University, Yonago) for technical assistance.

REFERENCES

1. Jopling, C., Sleep, E., Raya, M., Martí, M., Raya, A., and Izpisúa Belmonte, J. C. (2010) Zebrafish heart regeneration occurs by cardiomyocyte dedifferentiation and proliferation. *Nature* **464,** 606–609
2. Kikuchi, K., Holdway, J. E., Werdich, A. A., Anderson, R. M., Fang, Y., Egnaczyk, G. F., Evans, T., Macrae, C. A., Stainier, D. Y., and Poss, K. D. (2010) Primary contribution to zebrafish heart regeneration by gata4+ cardiomyocytes. *Nature* **464,** 601–605
3. Porrello, E. R., Mahmoud, A. I., Simpson, E., Hill, J. A., Richardson, J. A., Olson, E. N., and Sadek, H. A. (2011) Transient regenerative potential of the neonatal mouse heart. *Science* **331,** 1078–1080
4. Mollova, M., Bersell, K., Walsh, S., Savla, J., Das, L. T., Park, S.-Y., Silberstein, L. E., Dos Remedios, C. G., Graham, D., Colan, S., and Kühn, B. (2013) Cardiomyocyte proliferation contributes to heart growth in young humans. *Proc. Natl. Acad. Sci.* **110,** 1446–1451
5. Senyo, S. E., Steinhauser, M. L., Pizzimenti, C. L., Yang, V. K., Cai, L., Wang, M., Wu, T.-D., Guerquin-Kern, J.-L., Lechene, C. P., and Lee, R. T. (2013) Mammalian heart renewal by pre-existing cardiomyocytes. *Nature* **493,** 433–436
6. Erokhina, E. L. (1968) Proliferation dynamics of cellular elements in the differentiating mouse myocardium. *Tsitologiia* **10,** 1391–1409
7. Soonpaa, M. H., Kim, K. K., Pajak, L., Franklin, M., and Field, L. J. (1996) Cardiomyocyte DNA synthesis and binucleation during murine development. *Am. J. Physiol.* **271,** H2183–H2189
8. Toyoda, M., Shirato, H., Nakajima, K., Kojima, M., Takahashi, M., Kubota, M., Suzuki-Migishima, R., Motegi, Y., Yokoyama, M., and Takeuchi, T.

(2003) jumonji down-regulates cardiac cell proliferation by repressing cyclin D1 expression. *Dev. Cell* **5,** 85–97
9. Ikenishi, A., Okayama, H., Iwamoto, N., Yoshitome, S., Tane, S., Nakamura, K., Obayashi, T., Hayashi, T., and Takeuchi, T. (2012) Cell cycle regulation in mouse heart during embryonic and postnatal stages. *Dev. Growth Differ.* **54,** 731–738
10. Quelle, D. E., Ashmun, R. A., Shurtleff, S. A., Kato, J. Y., Bar-Sagi, D., Roussel, M. F., and Sherr, C. J. (1993) Overexpression of mouse D-type cyclins accelerates G_1 phase in rodent fibroblasts. *Genes Dev.* **7,** 1559–1571
11. Sherr, C. J., and Roberts, J. M. (1999) CDK inhibitors: positive and negative regulators of G1-phase progression. *Genes Dev.* **13,** 1501–1512
12. Tamamori-Adachi, M., Ito, H., Sumrejkanchanakij, P., Adachi, S., Hiroe, M., Shimizu, M., Kawauchi, J., Sunamori, M., Marumo, F., Kitajima, S., and Ikeda, M. A. (2003) Critical role of cyclin D1 nuclear import in cardiomyocyte proliferation. *Circ. Res.* **92,** e12–e19
13. Sohal, D. S., Nghiem, M., Crackower, M. A., Witt, S. A., Kimball, T. R., Tymitz, K. M., Penninger, J. M., and Molkentin, J. D. (2001) Temporally regulated and tissue-specific gene manipulations in the adult and embryonic heart using a tamoxifen-inducible cre protein. *Circ. Res.* **89,** 20–25
14. Heine, H. L., Leong, H. S., Rossi, F. M., McManus, B. M., and Podor, T. J. (2005) Strategies of conditional gene expression in myocardium: an overview. *Methods Mol. Med.* **112,** 109–154
15. Hogan, B., Beddington, R., Costanitini, F., and Lacy, E. (1994) Production of transgenic mice. in *Manipulating the Mouse Embryo* (Hogan, B., Beddington, R., Costanitini, F., and Lacy, E.m eds.) 2nd Ed., Cold Spring Harbor Laboratory Press, Plainview, NY
16. Motoyama, J., Kitajima, K., Kojima, M., Kondo, S., and Takeuchi, T. (1997) Organogenesis of the liver, thymus, and spleen is affected in jumonji mutant mice. *Mech. Dev.* **66,** 27–37
17. Takeuchi, T., Kojima, M., Nakajima, K., and Kondo, S. (1999) Jumonji gene is essential for the neurulation and cardiac development of mouse embryos with a C3H/He background. *Mech. Dev.* **86,** 29–38
18. Nakajima, K., Inagawa, M., Uchida, C., Okada, K., Tane, S., Kojima, M., Kubota, M., Noda, M., Ogawa, S., Shirato, H., Sato, M., Suzuki-Migishima, R., Hino, T., Satoh, Y., Kitagawa, M., and Takeuchi, T. (2011) Coordinated regulation of differentiation and proliferation of embryonic cardiomyocytes by a jumonji (Jarid2)-cyclin D1 pathway. *Development* **138,** 1771–1782
19. Shioya, T. (2007) A simple technique for isolating healthy heart cells from mouse models. *J. Physiol. Sci.* **57,** 327–335
20. Salic, A., and Mitchison, T. J. (2008) A chemical method for fast and sensitive detection of DNA synthesis *in vivo*. *Proc. Natl. Acad. Sci.* **105,** 2415–2420
21. Toyoda, M., Kojima, M., and Takeuchi, T. (2000) Jumonji is a nuclear protein that participates in the negative regulation of cell growth. *Biochem. Biophys. Res. Commun.* **274,** 332–336
22. Shirato, H., Ogawa, S., Nakajima, K., Inagawa, M., Kojima, M., Tachibana, M., Shinkai, Y., and Takeuchi, T. (2009) A Jumonji (Jarid2) protein complex represses cyclin D1 expression by methylation of histone H3-K9. *J. Biol. Chem.* **284,** 733–739
23. Tane, S., Ikenishi, A., Okayama, H., Iwamoto, N., Nakayama, K. I., and Takeuchi, T. (2014) CDK inhibitors, $p21^{Cip1}$ and $p27^{Kip1}$, participate in cell cycle exit of mammalian cardiomyocytes. *Biochem. Biophys. Res. Commun.* **443,** 1105–1109
24. Riabowol, K., Draetta, G., Brizuela, L., Vandre, D., and Beach, D. (1989) The cdc2 kinase is a nuclear protein that is essential for mitosis in mammalian cells. *Cell* **57,** 393–401
25. Ullah, Z., Kohn, M. J., Yagi, R., Vassilev, L. T., and DePamphilis, M. L. (2008) Differentiation of trophoblast stem cells into giant cells is triggered by p57/Kip2 inhibition of CDK1 activity. *Genes Dev.* **22,** 3024–3036
26. Nurse, P. (1990) Universal control mechanism regulating onset of M-phase. *Nature* **344,** 503–508
27. Solomon, M. J., Lee, T., and Kirschner, M. W. (1992) Role of phosphorylation in p34cdc2 activation: identification of an activating kinase. *Mol. Biol. Cell* **3,** 13–27
28. Honda, R., Ohba, Y., Nagata, A., Okayama, H., and Yasuda, H. (1993) Dephosphorylation of human p34cdc2 kinase on both Thr-14 and Tyr-15 by human cdc25B phosphatase. *FEBS Lett.* **318,** 331–334
29. Lindqvist, A., Källström, H., Lundgren, A., Barsoum, E., and Rosenthal, C. K. (2005) Cdc25B cooperates with Cdc25A to induce mitosis but has a unique role in activating cyclin B1-Cdk1 at the centrosome. *J. Cell Biol.* **171,** 35–45
30. Lee, G., White, L. S., Hurov, K. E., Stappenbeck, T. S., and Piwnica-Worms, H. (2009) Response of small intestinal epithelial cells to acute disruption of cell division through CDC25 deletion. *Proc. Natl. Acad. Sci.* **106,** 4701–4706
31. Lee, G., Origanti, S., White, L. S., Sun, J., Stappenbeck, T. S., and Piwnica-Worms, H. (2011) Contributions made by CDC25 phosphatases to proliferation of intestinal epithelial stem and progenitor Cells. *PLoS ONE* **6,** e15561
32. Motoyama, N., and Naka, K. (2004) DNA damage tumor suppressor genes and genomic instability. *Curr. Opin. Genet. Dev.* **14,** 11–16
33. Ciccia, A., and Elledge, S. J. (2010) The DNA damage response: making it safe to play with knives. *Mol. Cell* **40,** 179–204
34. Canman, C. E., Lim, D.-S., Cimprich, K. A., Taya, Y., Tamai, K., Sakaguchi, K., Appella, E., Kastan, M. B., and Siliciano, J. D. (1998) Activation of the ATM kinase by ionizing radiation and phosphorylation of p53. *Science* **281,** 1677–1679
35. Liu, Q., Guntuku, S., Cui, X.-S., Matsuoka, S., Cortez, D., Tamai, K., Luo, G., Carattini-Rivera, S., DeMayo, F., Bradley, A., Donehower, L. A., and Elledge, S. J. (2000) Chk1 is an essential kinase that is regulated by Atr and required for the G_2/M DNA damage checkpoint. *Genes Dev.* **14,** 1448–1459
36. Burma, S., Chen, B. P., Murphy, M., Kurimasa, A., and Chen, D. J. (2001) ATM phosphorylates histone H2AX in response to DNA double-strand breaks. *J. Biol. Chem.* **276,** 42462–42467
37. Ward, I. M., and Chen, J. (2001) Histone H2AX is phosphorylated in an ATR-dependent manner in response to replicational stress. *J. Biol. Chem.* **276,** 47759–47762
38. Sano, M., Minamino, T., Toko, H., Miyauchi, H., Orimo, M., Qin, Y., Akazawa, H., Tateno, K., Kayama, Y., Harada, M., Shimizu, I., Asahara, T., Hamada, H., Tomita, S., Molkentin, J. D., Zou, Y., and Komuro, I. (2007) p53-induced inhibition of Hif-1 causes cardiac dysfunction during pressure overload. *Nature* **446,** 444–448
39. Ciemerych, M. A., and Sicinski, P. (2005) Cell cycle in mouse development. *Oncogene* **24,** 2877–2898
40. Shiloh, Y. (2003) ATM and related protein kinases: safeguarding genome integrity. *Nat. Rev. Cancer* **3,** 155–168
41. Giono, L. E., and Manfredi, J. J. (2006) The p53 tumor suppressor participates in multiple cell cycle checkpoints. *J. Cell Physiol.* **209,** 13–20
42. Soonpaa, M. H., Koh, G. Y., Pajak, L., Jing, S., Wang, H., Franklin, M. T., Kim, K. K., and Field, L. J. (1997) Cyclin D1 overexpression promotes cardiomyocyte DNA synthesis and multinucleation in transgenic mice. *J. Clin. Invest.* **99,** 2644–2654
43. Pasumarthi, K. B., Nakajima, H., Nakajima, H. O., Soonpaa, M. H., and Field, L. J. (2005) Targeted expression of cyclin D2 results in cardiomyocyte DNA synthesis and infarct regression in transgenic mice. *Circ. Res.* **96,** 110–118
44. Gaussin, V., Van de Putte, T., Mishina, Y., Hanks, M. C., Zwijsen, A., Huylebroeck, D., Behringer, R. R., and Schneider, M. D. (2002) Endocardial cushion and myocardial defects after cardiac myocyte-specific conditional deletion of the bone morphogenetic protein receptor ALK3. *Proc. Natl. Acad. Sci.* **99,** 2878–2883
45. Eulalio, A., Mano, M., Dal Ferro, M., Zentilin, L., Sinagra, G., Zacchigna, S., and Giacca, M. (2012) Functional screening identifies miRNAs inducing cardiac regeneration. *Nature* **492,** 376–381
46. Mahmoud, A. I., Kocabas, F., Muralidhar, S. A., Kimura, W., Koura, A. S., Thet, S., Porrello, E. R., and Sadek, H. A. (2013) Meis1 regulates postnatal cardiomyocyte cell cycle arrest. *Nature* **497,** 249–253
47. Oberpriller, J. O., and Oberpriller, J. C. (1974) Response of the adult newt ventricle to injury. *J. Exp. Zool.* **187,** 249–253
48. Poss, K. D., Wilson, L. G., and Keating, M. T. (2002) Heart regeneration in zebrafish. *Science* **298,** 2188–2190